






Original Article


Effects of solar radiation and fine roots on suction of *Amorpha fruticose*-vegetated soil


GUO Han-qing^{1,2}  <https://orcid.org/0000-0001-5809-6322>; e-mail: guohanqing20@mails.ucas.ac.cn


CHEN Xiao-qing^{1,2*}  <https://orcid.org/0000-0002-0177-0811>;  e-mail: xqchen@imde.ac.cn

SONG Dong-ri^{1,2}  <https://orcid.org/0000-0001-6892-9770>; e-mail: drsong@imde.ac.cn

MU Qing-yi³  <https://orcid.org/0000-0002-9235-4978>; e-mail: qingyimu@mail.xjtu.edu.cn

SADEGHI Hamed⁴  <https://orcid.org/0000-0002-3453-9309>; e-mail: hsadeghi@sharif.edu

JIANG Hao^{1,2}  <https://orcid.org/0000-0002-7541-8482>; e-mail: jianghao@imde.ac.cn

LV Ming^{1,2}  <https://orcid.org/0000-0002-0695-5305>; e-mail: lvming20@mails.ucas.ac.cn

*Corresponding author

¹ Laboratory of Mountain Hazards and Earth Surface Process/Institute of Mountain Hazards and Environment, Chinese Academy of Sciences, Chengdu 610299, China

² University of Chinese Academy of Sciences, Beijing 100049, China

³ Department of Civil Engineering, Xi'an Jiaotong University, Xi'an 710049, China

⁴ Department of Civil Engineering, Sharif University of Technology, Tehran 145889694, Iran

Citation: Guo HQ, Chen XQ, Song DR, et al. (2023) Effects of solar radiation and fine roots on suction of *Amorpha fruticose*-vegetated soil. Journal of Mountain Science 20(6). <https://doi.org/10.1007/s11629-022-7694-x>

© Science Press, Institute of Mountain Hazards and Environment, CAS and Springer-Verlag GmbH Germany, part of Springer Nature 2023

Abstract: The thickness of shallow landslides is generally less than 2 m, which is of the same order of magnitude as the growth range of vegetation roots. Vegetation roots can improve the stability of shallow soil through mechanical and hydraulic effects. Therefore, the landslide process is closely related to the plant roots growing on the slope surface. Plant roots play a dominant role in the regulation of soil suction through solar radiation induced transpiration. However, little is known about the correlation between cumulative solar radiation and soil suction. Moreover, the specific effects of fine roots on the suction distribution are not clear in most previous studies. In this study, a vegetated soil of a drought-tolerant and water-tolerant shrub, namely *Amorpha fruticose*, was adopted. The suction and volumetric

water content of bare and vegetated soils were monitored under natural conditions for 4 months. The results demonstrate that there is a nearly linear relationship between cumulative solar radiation and suction ranging from zero to 100 kPa. Regarding the modeling of the soil-plant-atmosphere interactions, this relationship could serve a significant role in calculating the root water uptake under given solar radiation conditions. In addition, higher suctions were observed at the lower layer of the vegetated soil than those at the middle layer, which is different from the results of vegetated soil from previous investigations. This is due to the fact that the root area index (RAI) of fine roots at the lower layer is twice that of the middle layer. Importantly, the higher concentration of fine roots at the lower layer of vegetated soil sample resembles the root distribution of shrub near the soil-bedrock interface on shallow bedrock landslides. The fine roots would increase soil

Received: 06-Sep-2022

Revised: 13-Oct-2022

Accepted: 16-Dec-2022

suction through transpiration, and hence reduce the permeability and increase shear strength of landslides. Eventually, these new findings serve as a preliminary step on the evaluation of the stability of this common type of landslides.

Keywords: Field monitoring; Fine roots; Solar radiation; Suction; Shallow bedrock landslide

1 Introduction

Shallow landslides are natural geomorphic processes that shape the landscape and are commonly triggered by rainstorms (Rickli and Graf 2009) or earthquakes (Croissant et al. 2019). As a green and ecologically-balanced reinforcement approach (Pollen et al. 2004; Ng and Menzies 2007; Jin et al. 2019), vegetated slope not only restrains the surface soil from erosion (Zhang et al. 2020), but also improves the stability of shallow soil through mechanical and hydraulic effects (Waldron 1977; Pollen et al. 2004; Feng et al. 2020; Ng et al. 2020a; Su et al. 2020). Mechanical effects mainly include reinforcing effect of fibrous roots, anchoring effect of taproot, and pulling effect of horizontal roots (Greenway 1987; Pollen et al. 2004; Stokes et al. 2009). In terms of hydraulic effects, vegetation can increase soil suction through transpiration, which is beneficial for reducing permeability and increasing shear strength of unsaturated soils (Ng and Menzies 2007; Ng 2017; Ni et al. 2018; Sadeghi and Ng 2018; Mu et al. 2022). Very often, the growth depth of woody roots is approximate to the thickness of shallow landslides. Therefore, the roots of woody plants on the slope have a significant influence on the stability of shallow landslides.

The transpiration-induced suction depends on root water uptake, which is a complicated process due to the soil–plant–atmosphere interactions (Segal et al. 2008; Nyambayo and Potts 2010). Accurate prediction of the suction changes induced by transpiration in the numerical simulations requires an understanding of the physical mechanism of radiation-transpiration effects on water uptake and suction response. Therefore, a quantified relationship between solar radiation and suction could be of vital importance for the numerical simulations on this area. Most root water uptake models, which have been implemented into finite element codes (Indraratna et al. 2006; Nyambayo and Potts 2010; Zhu et al. 2018),

adopted soil suction, root distribution, and potential transpiration as input parameters. The influences of atmospheric conditions, i.e., the solar radiation, temperature, and humidity, are not clear. Although solar radiation is one of the key external driving factors in transpiration-induced suction (Allen et al. 1998), little is known about the correlation between solar radiation and transpiration-induced suction.

The aboveground vegetative leaf and atmospheric conditions, as well as the belowground root and soil environments, together determine the intensity of transpiration (Haseba and Takechi 1972; Pieruschka et al. 2010). The aboveground external factors affecting transpiration depend mainly on the difference in vapor pressure inside and outside of the leaf and the magnitude of stomatal diffusion resistance (Haseba and Takechi 1972; Pieruschka et al. 2010; Lin et al. 2016). Other things being equal, solar radiation controls vegetation transpiration (Singh et al. 1982; Ta et al. 2011). On one hand, solar radiation causes the opening of stomata and reduces stomatal resistance, thus enhancing transpiration (Singh et al. 1982; Baille et al. 1994; Pieruschka et al. 2010). On the other hand, solar radiation increases the temperature of the atmosphere and leaves, and decreases the relative humidity of the air, which increases the vapor pressure difference inside and outside of the leaves and accelerates transpiration rate (Haseba and Takechi 1972; Lin et al. 2016). Water in the soil is sequentially evaporated to the atmosphere by vegetation transpiration through root hairs, intra-root ducts, intra-stem ducts, intra-leaf ducts, stomata, and finally the atmosphere (Allen et al. 1998). This means that transpiration of vegetation directly influences the buildup of soil suction through the root system.

The root is the organ of vegetation for uptaking water from the soil, and its morphology along the soil depth has a significant effect on the distribution of soil suction (Zhu et al. 2018; Ni et al. 2018). For coarse roots (diameter > 2 mm), the liquid water inside the root is easily vaporized to generate air bubbles under high negative pressure. The number of channels for the flow of liquid water are reduced, and the permeability becomes low, adversely affecting the root water uptake. On the contrary, the fine roots (diameter < 2 mm) have a larger contact area with the soil, and their epidermis and water conduits have higher permeability (Segal et al. 2008), which is more conducive for root water uptake. It is understood from

the current literatures that, most previous studies focused on the effect of overall root characteristics (characterized by root area index (RAI) and root length density (RLD), etc.) on soil suction (Scholl et al. 2014; Lu et al. 2020; Ng et al. 2016, 2020b). The effect of fine roots, especially fine roots of shrub, has not been fully explored.

Soil-water characteristics mainly depend on void ratio, overburden stress, and soil pore size distribution (Romero et al. 1999; Ng and Pang 2000; Sadeghi et al. 2016; Mu et al. 2020; Ng et al. 2022a). Experimental studies (Scholl et al. 2014; Ng et al. 2016; Jotisankasa and Sirirattanachat 2017; Ni et al. 2018) have shown that root system can modify the structure of soil and thus affect the soil-water characteristics. Roots change soil structure mainly through (i) volumetric occupancy of roots in soil pore space (Scanlan and Hinz 2010; Scholl et al. 2014); (ii) the release of exudates from roots to clog fine pores (Grayston et al. 1997; Traore et al. 2000); and (iii) shrinkage or decay of coarse roots is conducive to the formation of macro-pores (Ghestem et al. 2011; Ni et al. 2018). Fine and coarse roots affect the soil structure in different ways. Fine roots have a pore-clogging effect on the soil, causing small aggregates to coalesce. Coarse roots cause relatively large movements and rearrangements of soil particles and create fissures in the soil (Bodner et al. 2014; Lu et al. 2020). Herbaceous plants and shrubs have different root thicknesses, root distribution patterns along depth, and root reinforcement mechanisms for slopes. Most of current studies are based on herbaceous plants and there lacks an understanding of the role of shrub roots in modifying soil-water characteristics.

Based on the research gaps of the above studies, the aim is to study the effects of solar radiation and fine roots on suction of shrub-vegetated soil. To achieve the main objectives of this research, the suction and volumetric water content of bare soil and *Amorpha fruticosa* vegetated soil were continuously monitored in the field for 4 months. The roots of vegetated soils monitored in parallel were

excavated and their root area index (RAI) was measured. The effects of cumulative solar radiation on suction were investigated, and the contribution of fine roots to the distribution of soil suction was analyzed. Finally, the influence of plant roots on soil-water characteristics through their modification of soil structure was further investigated.

2 Monitoring of Shrub-Vegetated Soil

2.1 Monitoring site and climate

The monitoring of shrub-vegetated soil was carried out in Yanting Agro-ecological Experiment Station of Purple Soil, Chinese Academy of Sciences. The site is located at Linshan town, Yanting county, China (105°27'E, 31°16'N), and it belongs to the subtropical humid monsoon climate zone. Site climate conditions, which come from the long-term monitoring data of the network on the station, including temperature, relative humidity, solar radiation, and rainfall intensity, were measured continuously by an automatic weather station. During the monitoring period (from 17 June 2021 to 23 October 2021), the temperature ranged from 17°C to 39°C and the relative humidity varied from 28% to 100%. The maximum rainfall intensity was 29 mm/h. The solar radiation ranged from 0 to 3.65 MJ/(m²·h).

2.2 Monitoring setup and instrumentation

Fig. 1 shows the schematic diagram of plan and cross-sectional views of a vegetated test cylinder. The

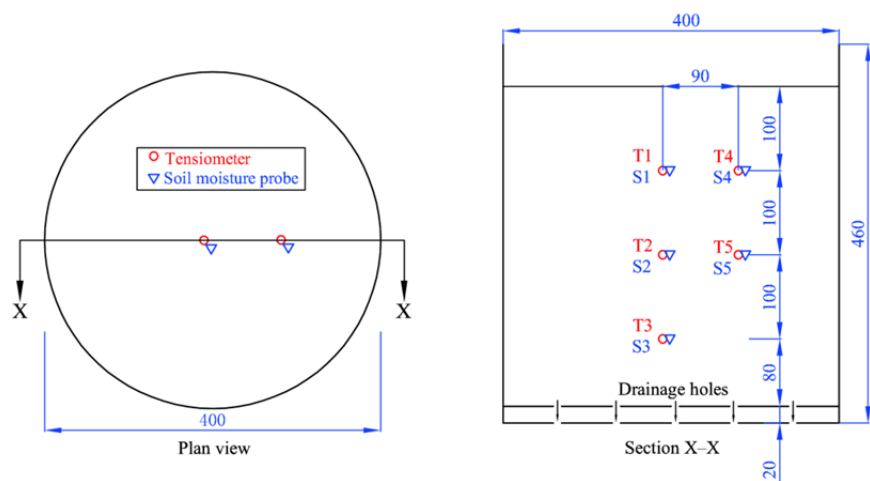


Fig. 1 Schematic diagram of plan and cross-sectional views of a vegetated test cylinder (all dimensions in mm).

cylinder is made of polyvinyl chloride (PVC), and is characterized with diameter of 400 mm and height of 460 mm. Soil was compacted in each cylinder and an individual seedling was transplanted in the center. The lateral boundaries were impermeable, while the bottom boundary was subjected to drainage through holes drilled to the base plate. The top boundary was subjected to atmospheric condition. The soil column is 380 mm in height.

In order to measure the responses of suction, two vertical arrays of miniature-tip tensiometers (Model 2100F, Soil moisture Equipment Corp) were installed along the soil depth (Fig. 1). Each one has a ceramic cup (*i.e.*, the sensing element) of 6 mm in diameter and 25 mm in length. The accuracy of each tensiometer is ± 1 kPa. The vacuum dial gauge of the 2100F tensiometer was replaced with a pore pressure transducer (PPT), so that the suction data can be collected automatically (Sadeghi et al. 2020). Prior to installation, the ceramic tip of each tensiometer was fully saturated and the plastic tube was completely filled with air-free water, as cavitation could occur in each tensiometer when suction approached 80 kPa. After installation, any gap between probe and surrounding soil was backfilled with soil paste to prevent preferential water flow during monitoring.

One vertical array, consisting of three tensiometers (denoted T1, T2, and T3 in Fig. 1), was installed directly beneath the shrub seedling located in the middle of the cylinder. The instrument depths were 100, 200, and 300 mm from the soil surface, respectively. Another vertical array, consisting of two tensiometers (denoted T4 and T5 in Fig. 1), was installed at 90 mm from the centerline of cylinder. The instrument depths were 100 and 200 mm from the soil surface. During the monitoring period, whenever the suction increases to about 60 kPa, a large amount of air bubbles will be entrapped in the plastic tube of tensiometers. At this time, it is necessary to release the trapped air and refill the plastic tube with air-free water.

Five soil moisture probes (EC-5, Decagon Devices, Inc) were installed next to the five tensiometers to monitor volumetric water content (VWC). They were denoted S1 to S5 in Fig. 1. The purposes of moisture probes were to check the measurements of suction against VWC and to investigate the effects of roots on soil-water characteristics. Each moisture probe was calibrated in the laboratory using the same soil in the monitoring cylinder and the accuracy was found to be

$\pm 1\%$ of VWC. Both the suction and volumetric water content were continuously collected by a data logger (cRIO-9040, National Instruments), one data point every two minutes.

2.3 Soil and plant type

The soil selected for investigation is commonly found in Yanting Agro-ecological Experiment Station of Purple Soil. The dry density of soil was controlled at 1.28 g/cm^3 , which was consistent with the surrounding cultivated land. Measurements of the particle-size distribution show that the contents of gravel, sand, silt and clay in the soil are 0.6%, 31.7% and 67.7%, respectively. The coefficients of uniformity and curvature are found to be 9.2 and 1.5 respectively, and this soil is thus classified as a well-graded soil. The plastic limit and liquid limit of the test soil are 16% and 30%, respectively. Based on the measured particle-size distribution (Fig. 2) and Atterberg limits, and following the Unified Soil Classification System (USCS; ASTM, 2017), the soil is classified as lean clay (CL). Other measured properties of the soil are summarized in Table 1.

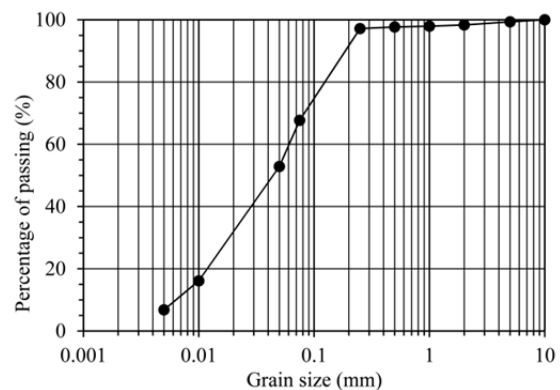


Fig. 2 Grain size distribution of the test soil.

The vegetation selected for investigation is a drought-tolerant and water-tolerant shrub species, *Amorpha fruticosa*. This shrub is selected because (i) it has a thick taproot and a lot of lateral roots; (ii) the soil requirements of this species are not strict, and it can grow on barren hillsides, roadsides, and river banks; and (iii) it can grow rapidly with dense branches and leaves. Based on these advantages, it is an outstanding shrub species for slope protection.

2.4 Test program

In this study, five shrub seedlings, which were previously grown in a nursery, were transplanted to five separate cylinders at mid-April 2021. Each vegetated cylinder was irrigated every ten days for one month. The duration of one month of frequent irrigation schedule was sufficient for plant roots to establish with the surrounding soil. Due to the variability of shrub species, the five shrub seedlings had different properties. They had a mean height of 823 mm with standard error of 38 mm at mid-June, and a mean height of 2113 mm with standard error of 51 mm when excavated on October.

Two of these five vegetated cylinders were used for monitoring suction and volumetric water content with tensiometers and soil moisture probes, denoted as V1 and V2. The remaining three cylinders that were used as a control group are denoted as V3, V4, and V5, which would be used to measure RAI. For comparison, tensiometers and soil moisture probes were installed on one cylinder of bare soil, which was denoted as B. The monitoring program was summarized in Table 2.

2.5 Test procedures

All six cylinders were exposed to the natural environment for 6 months from 17 April 2021 to 23 October 2021. For the first 2 months after transplantation, the probes and plant roots were not tightly connected to the soil, so the monitoring was not performed. The monitoring period is carried out for 4 months, from 17 June 2021 to 23 October 2021, during which suction and volumetric water content were monitored continuously.

The distribution of root has a significant effect on the level of soil suction along depth. At early October, three cylinders of parallel vegetated soils (V3, V4, and V5, the total number is $m=3$), with similar basal stem and plant height to V1 and V2, were excavated to measure the root parameters. This was achieved by carefully excavating the entire soil-root assembly. Afterwards, the whole root system was photographed and cut into four sections along the vertical direction, and the lengths of each section were 100 mm, 100 mm, 100 mm, and 80 mm, respectively. The root was scanned with Microtek root scanner (Zhejiang Top Yunnong Technology Co., Ltd.), and the length, diameter, surface area, and volume of the root were calculated with RhizoPheno analysis software to obtain the root area index (RAI). Hence, in this study, RAI was discretized at intervals of 100 mm. Because

Table 1 Index properties of test soil

Index properties	Value
Particle-size distribution	
Gravel content (4.75-75 mm, %)	0.6
Sand content (0.075-4.75 mm, %)	31.7
Silt & Clay content (< 0.075 mm, %)	67.7
Effective particle size D_{10} (mm)	0.007
Median particle size D_{30} (mm)	0.030
Controlled particle size D_{60} (mm)	0.060
Coefficient of uniformity (D_{60}/D_{10})	9.2
Coefficient of curvature ($D_{30}^2/(D_{60}D_{10})$)	1.5
Specific gravity	2.65
Atterberg limits	
Plastic limit (%)	16
Liquid limit (%)	30
Plasticity index	14
Unified Soil Classification System (USCS)*	Lean clay (CL)

Notes: * ASTM (2017).

Table 2 Monitoring program

Test ID	Monitoring period for analysis and soil-root parameters					
	25-Jun. to 05-Jul.		04-Sep. to 12-Sep.		18-Sep. to 01-Oct.	
B	Suction	VWC	Suction	VWC	Suction	VWC
V1	Suction	VWC	Suction	VWC	Suction	VWC
V2	Suction	VWC	Suction	VWC	Suction	VWC
V3	/	/	/	/	RAI	
V4	/	/	/	/	RAI	
V5	/	/	/	/	RAI	

Notes: VWC: volumetric water content; RAI: root area index.

of their similar growth, the average RAI of these three cylinders was adopted to represent that of instrumented V1 and V2.

The root area index (RAI) is a dimensionless index that indicates the water uptake ability of roots within the root zone. The RAI is defined as the ratio of the root surface area in a longitudinal section at a specific depth to the area of the root extension area in the horizontal direction. RAI can be expressed as

$$RAI = \frac{\sum_{i=1}^n \pi d_i \Delta h}{\pi D_r^2 / 4} \quad (1)$$

where, Δh is the calculated depth range, usually 10 mm; D_r is the maximum extension diameter of the root system in the horizontal direction; d_i is the diameter of the i -th root system; and n is the total number of roots.

The global of root morphology of *Amorpha fruticose* (Fig. 3a) is almost rectangular, which is due to the restriction of the cylinder. Note that the root system in the figure stretches out in excess of 400 mm,

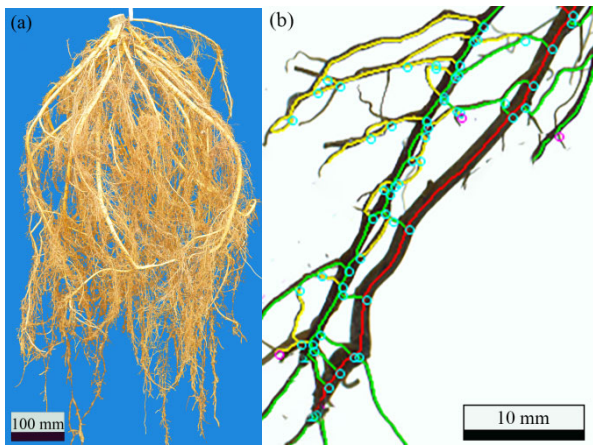


Fig. 3 Root system of *Amorpha fruticosa*: (a) the root morphology; (b) the details of the root system analysis: the taproot (red), the first lateral roots (green), and secondary lateral roots (yellow). The pink circle is the tip of the root, and the green circle is branching point.

which is caused by the sagging of the fine roots under the weight of gravity. Fig. 3b shows the details of the root system analysis. Significant differences were assessed with one-way ANOVA (analysis of variance), followed by post hoc Tukey’s test. Correlations were tested using regression analysis. Results were considered statistically significant when $p < 0.05$. Each suction data point is derived from monitoring data over a 24-hour period. There is some error in the root analysis. For example, some fine roots are not counted, which would lead to the actual fine roots will be more than the analyzed result.

3 Interpretation of Measured Results

3.1 Observed RAI profiles of root

Fig. 4 depicts the measured profile of RAI along the soil depth of all three shrub individuals. It is note that the data points at 100 mm, 200 mm, and 300 mm depths in the figure refer to the RAI of roots determined within the depth ranges of 50–150 mm, 150–250 mm, and 250–350 mm, respectively.

It can be seen that at depths of 100 mm, 200 mm, and 300 mm, the RAI of fine roots accounts for 52%, 58%, and 75% of root classes at each depth, respectively. This means that the RAI of fine roots is greater than that of coarse roots, regardless of the depth at which they are located. The RAI of fine roots at the 300 mm depth is 81% and 83% greater than that at depths of 100 mm and 200 mm, respectively. On the one hand, the newborn fine roots tend to grow

downwards, resulting in fewer fine roots at the upper layer of soil. On the other hand, a large number of roots are restricted to grow and much fine roots accumulate at the lower layer. The p -value for RAI of fine roots with diameter of 0-2.00 mm is 0.002 at three depths, the difference was significant (Table 3). The RAI of fine roots at 300 mm are significantly different from those at 100 mm and 200 mm, respectively. It is also visually obvious from Fig. 3a that the fine roots at the lower layer is denser than those at the middle and upper layers, respectively.

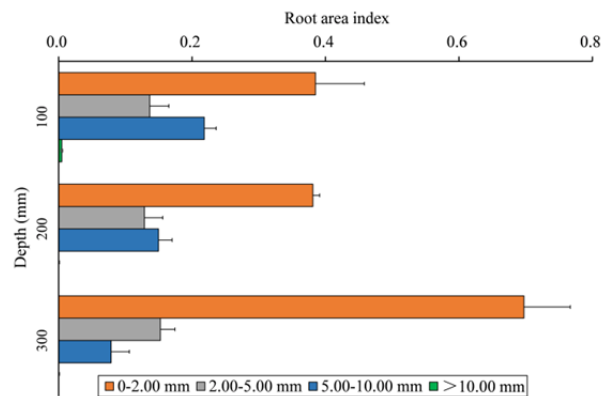


Fig. 4 Distribution of root area index (RAI) along soil depth. Mean values are reported as mean \pm standard error ($m = 3$).

Table 3 Summary of root area index (RAI) at three depths (mean \pm standard error, $m = 3$)

Diameter classes (mm)	Depth (mm)			p-value
	100	200	300	
0.00-2.00	0.38 \pm 0.07a	0.38 \pm 0.01a	0.70 \pm 0.07b	0.002
2.00-5.00	0.14 \pm 0.03a	0.13 \pm 0.03a	0.15 \pm 0.02a	0.810
5.00-10.00	0.22 \pm 0.02b	0.15 \pm 0.02ab	0.08 \pm 0.03a	0.013
>10.00	0.00 \pm 0.00a	0.00 \pm 0.00a	0.00 \pm 0.00a	0.422

3.2 Responses of suction and volumetric water content to evapotranspiration

The suction and water content responses of vegetated soils (V1 and V2) were similar, so only the case of V1 was shown in Fig. 5. The lack of data during the period was mainly caused by malfunction of the acquisition system. The variation of suction and volumetric water content of bare soil B along soil depth is negligible. The suction and volumetric water content at depth of 100 mm are adopted to represent the entire cylinder, denoted as B-T1 and B-S1. During the no-rainfall periods, apparent peaks of suction were recorded due to the significant evapotranspiration (Fig. 5a). Accordingly, the water content dropped to its minimum (Fig. 5b). In general, the variation of suction along depth was not obvious,

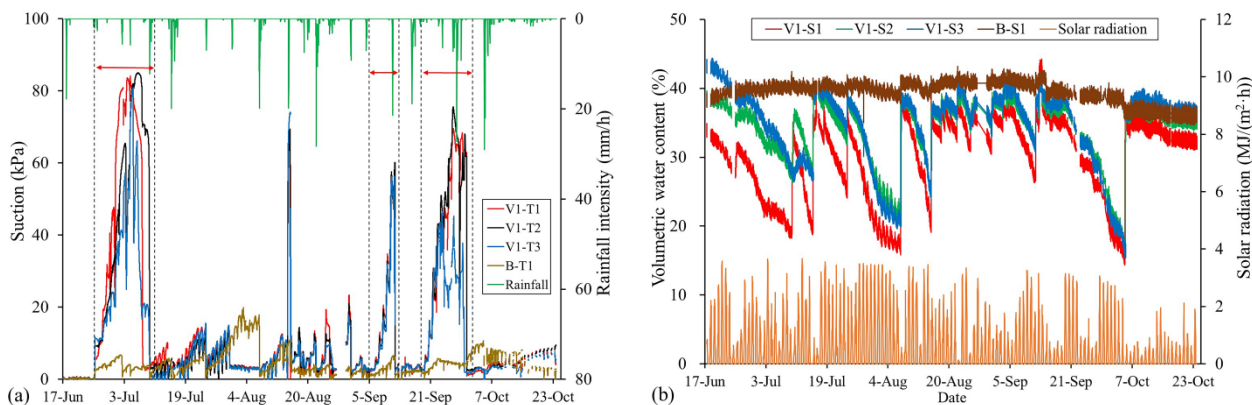


Fig. 5 Suction (T) and volumetric water content (S) responses of bare soil B and vegetated soil V1, regulated by the site climate during the entire monitoring period: (a) suction and rainfall intensity (the intervals marked with red arrows are the major analyzed periods); (b) volumetric water content and solar radiation.

but the variation of volumetric water content along depth was more pronounced.

When subjected to rainfall, solar radiation is minimal. Accordingly, the suction decreased and volumetric water content rose rapidly for vegetated soil. Compared to vegetated soil, the magnitude of the variation in suction and volumetric water content of bare soil was not significant, only one-tenth of the former. Three periods, from 25 June to 05 July, from 04 to 12 September, and from 18 September to 01 October (marked with red arrows in Fig. 5a) were chosen for detailed analysis of the relationship between induced suction and cumulative solar radiation, the suction distribution along soil depth, and soil-water characteristics, because of their large and representative magnitude of variation.

3.3 Relationship between induced suction and cumulative solar radiation

The solar radiation determines the aboveground plant transpiration to a large extent. While the underground plant roots (mainly fine roots) uptake water from the soil during transpiration, resulting in an increase in suction. The suction responses of vegetated soil (V1) and bare soil are compared to highlight the effect of solar radiation on suction buildup (Fig. 6). The suction at B-T1 is adopted to represent the suction variation of bare soil, since the suction buildup of B-T1 due to evaporation is the fastest compared to those measured at other locations. The suction of bare soil rises slowly compared to vegetated soil due to the lack of transpiration. It is interesting to note that, during the day, suction increases with the cumulative solar radiation. At night,

when solar radiation is absent, suction plateaus without increasing, or even decreases due to the redistribution of soil moisture, with a capillary effect from area of high to low moisture.

During each of three monitoring periods (eight-ten days), the leaf area index and root characteristics were considered unchanged. Therefore, the solar radiation energy interception rate of the leaves remained constant. Despite the ratcheting effect caused by the day-night cycles, the suction of vegetated soil V1 increases with the cumulative solar radiation in all three time periods and shows a linear relationship, which is significant with fairly good correlations ($p < 0.001$, $R^2 > 0.9$, Fig. 7). However, this relationship is not unconstrained, because the root water uptake intensity would decrease at the high suction range. The transpiration reduction function $\alpha(h)$, which is the relationship between the ratio of actual to potential maximum transpiration rate and soil suction, describes an empirical non-linear root water uptake model (Feddes et al. 1978, Fig. 8). The four values of suction in the reduction function change with the type of soil, the type of vegetation, and its growth state. For most types of vegetation, $0 < h_1 < h_2 < h_3 < 100$ kPa, and $h_4 > 100$ kPa. Root water uptake is nearly constant when suction is lower than the threshold suction, h_3 . According to Fig. 7 and Fig. 8, this linear relationship may only apply in the range below 100 kPa, which is the range where most vegetation grows normally. As suction exceeds h_3 , root water uptake would reduce with suction (Feddes et al. 1978; van Genuchten 1987). The linear relationship between suction and cumulative solar radiation at the suction range higher than 100 kPa remains uninvestigated.

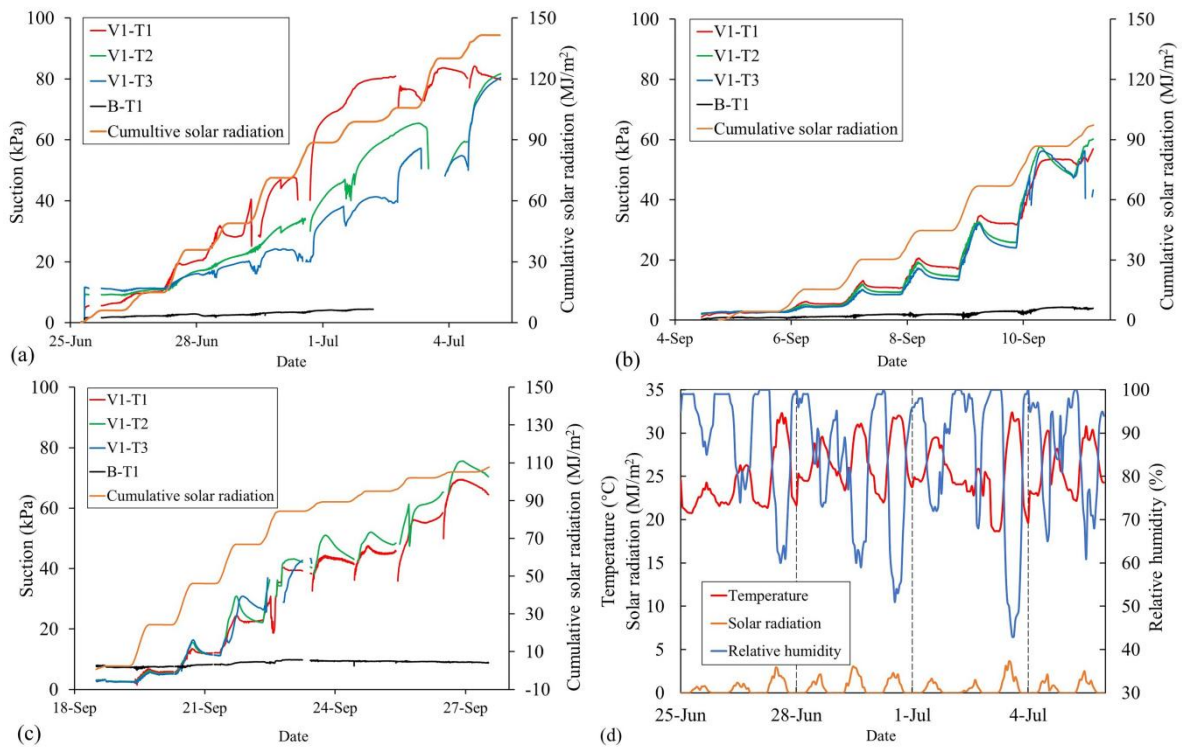


Fig. 6 Variations in suction (T) and cumulative solar radiation for bare soil B and vegetated soil V1: (a) from 25 June to 05 July; (b) from 04 to 12 September; (c) from 18 September to 01 October; and (d) changes of solar radiation, temperature, and relative humidity measured at every hour (from 25 June to 05 July).

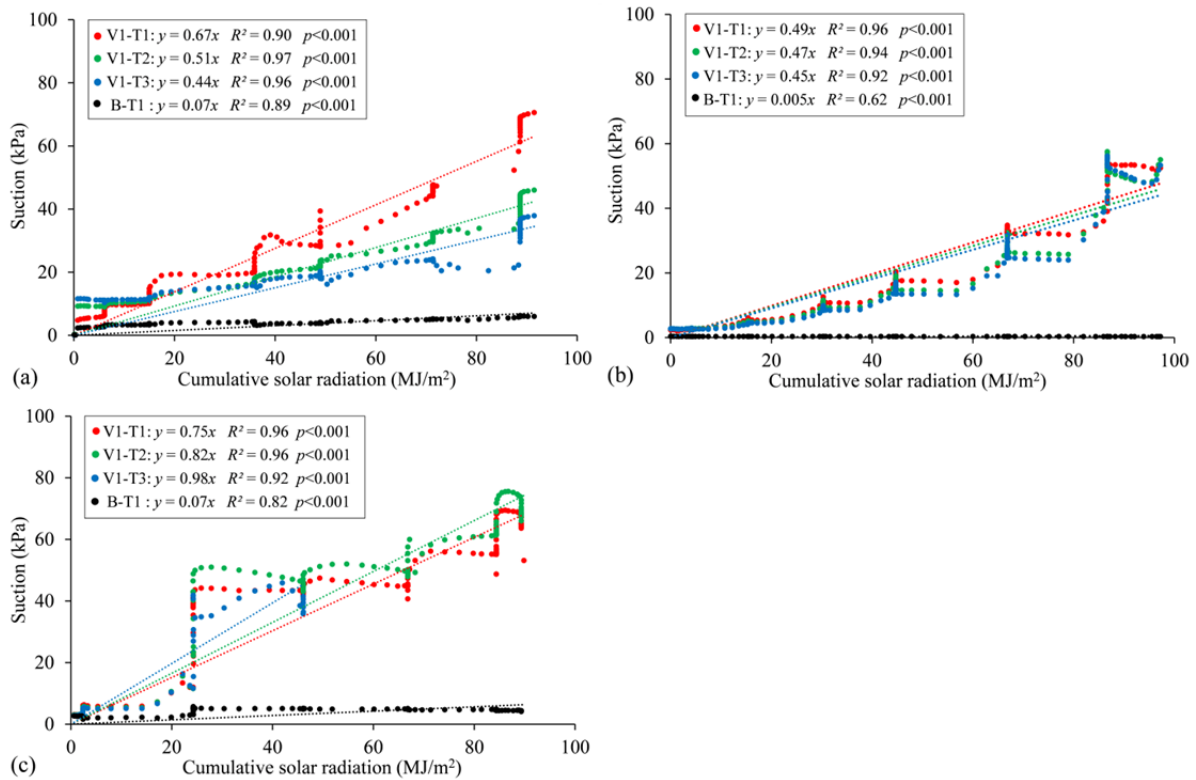


Fig. 7 Relationship between suction (T) and cumulative solar radiation for bare soil B and vegetated soil V1: (a) from 25 June to 05 July; (b) from 04 to 12 September; and (c) from 18 September to 01 October.

From Fig. 7, it can be seen that the slope of the relationship between cumulative solar radiation and suction changes at different depths in three growth periods. In the first growth period, the slope is $T_1 > T_2 > T_3$. That is, the suction distribution along soil depth is $T_1 > T_2 > T_3$ for the same cumulative solar radiation (Fig. 7a). This is because, at the early stage, the root mainly grows at the upper middle T_1 and T_2 , where the root water uptake is stronger, and there is also evaporation at T_1 . In the second stage, the slope at the three depths is close (Fig. 7b). This is because the roots extend downward to the lower layer, which increases the root water uptake intensity at T_3 . In the third stage, the slope is $T_3 > T_2 > T_1$ (Fig. 7c). The large amount of fine roots cluster in the lower layer of the soil cause a strong root water uptake intensity at T_3 and quick suction buildup. This indicates that the root distribution and solar radiation affect the soil suction in a coupled manner.

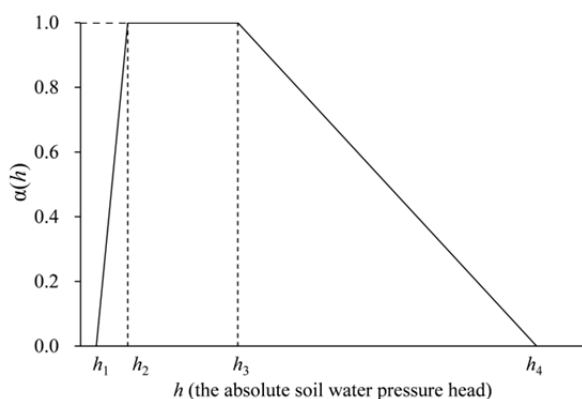


Fig. 8 Transpiration reduction function $\alpha(h)$ adopted for simulating root-water uptake (Feddes et al. 1978, for illustrating the upper limit of the linear relationship between suction and cumulative solar radiation)

3.4 Relationship between induced suction and RAI of fine roots

The suction distribution along soil depth of bare soil (B) and vegetated soil (V1 and V2) were analyzed in detail for the three periods selected above (Figs. 9&10). The suction distribution along depth is shown for a selection of specific moments. For vegetated soil V1, from 25 June to 04 July, the suction distribution along soil depth is $T_1 > T_2 > T_3$ (Fig. 9a). From 06 to 10 September, the difference in suction distribution along soil depth disappears. The suction is almost uniformly distributed along soil depth (Fig. 9b).

The roots of *Amorpha fruticosa* were excavated

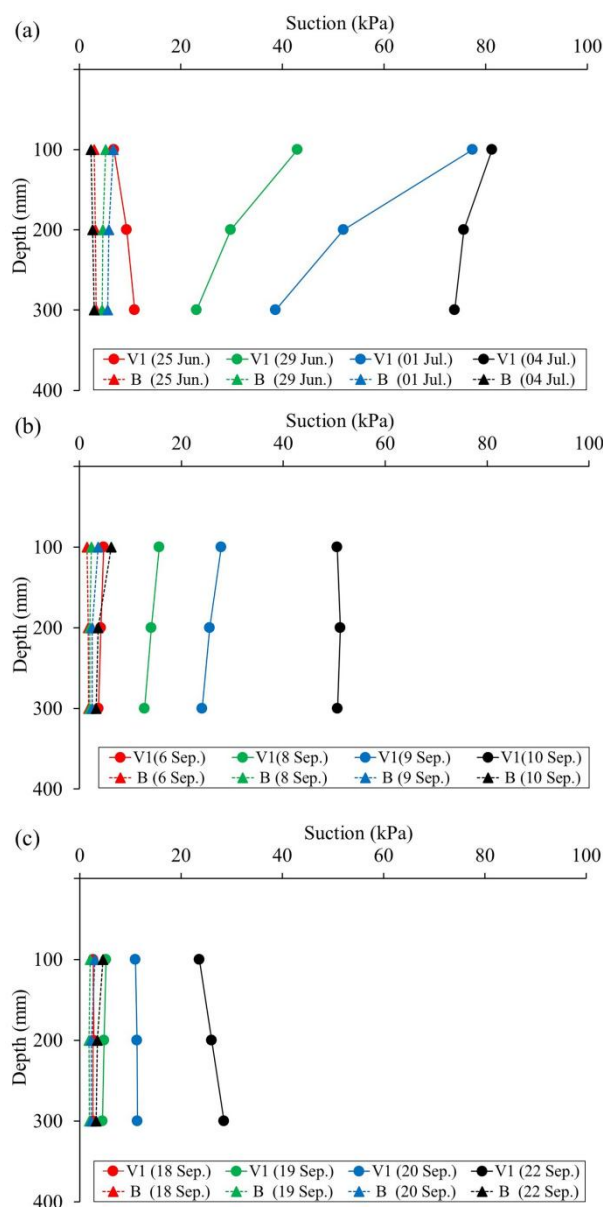


Fig. 9 Suction distribution along soil depth of bare soil B and vegetated soil V1: (a) from 25 June to 05 July; (b) from 04 to 12 September; and (c) from 18 September to 01 October (The standard error is so small that the error line is obscured).

and RAI was measured at early October, so that the suction distribution from 18 September to 22 September (Fig. 9c) can be explained through the measured RAI. The RAI of fine roots at 300 mm is the highest (Fig. 4), resulting in a fast rise in suction. This explains the highest suction at the lower layer and further confirms that the larger the root area index (RAI) of fine roots, the more favorable it is for the roots to uptake water. The soil at 100 mm depth is at the upper layer, which is open to the air and has a

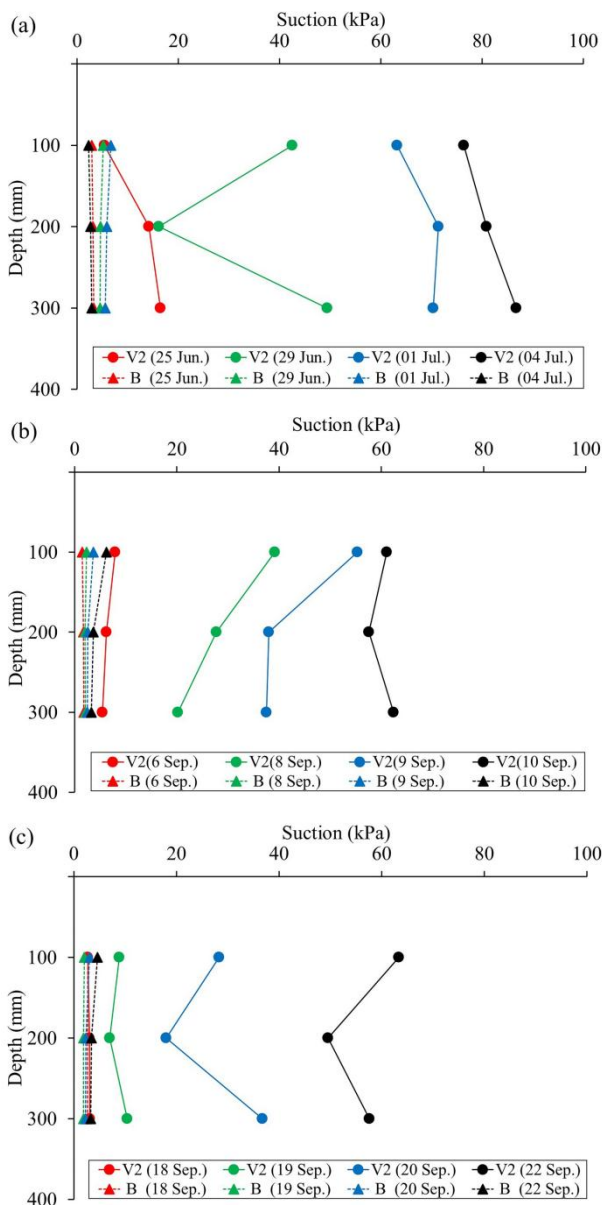


Fig. 10 Suction distribution along soil depth of bare soil B and vegetated soil V2: (a) from 25 June to 05 July; (b) from 04 to 12 September; and (c) from 18 September to 01 October (The standard error is so small that the error line is obscured).

higher evaporation rate, which also makes the suction at this area of the vegetated soil higher.

Despite the RAI for the periods from 25 June to 04 July and from 06 to 10 September is not available, it is postulated that the suction distribution (Fig. 9a&b) is caused by the evolution of fine roots along the soil depth. Specially, for the period from 25 June to 04 July (2 months after transplantation), the fine roots mainly concentrate at the upper and middle layers. In combination with the evaporation from the

upper layer, the maximum suction appears at the upper layer (Fig. 9a). As the fine roots further extends downwards to the deeper soil (e.g., the period from 06 to 10 September, 5 months after transplantation), the fine roots start to uptake more water from the lower layer, resulting in a uniform distribution of suction (Fig. 9b). Finally, in the last stage (from 18 September to 22 September), as revealed by RAI in Fig. 4, fine roots concentrate at the lower layer and suction peaks there accordingly.

For vegetated soil V2, from 25 June to 04 July, the suction distribution along soil depth is $T_3 > T_1$ (Fig. 10a), while the suction fluctuates more at 200 mm. From 06 to 10 September, the suction distribution along soil depth is $T_1 > T_2 > T_3$ in the early stage of drying. By the late stages of drying, the suction distribution along soil depth is $T_1 > T_3 > T_2$ (Fig. 10b). From 18 September to 22 September, the suction at depths of 300 mm and 100 mm are greater than that at depth of 200 mm (Fig. 10c). The greater the RAI is, the more intense the transpiration and the more favorable for the roots to uptake water. In turn, the volumetric water content of the soil at the maximum RAI (300 mm) (Fig. 4a) decreases more quickly, resulting in a faster rise in suction. Note the pattern of suction distribution for V2 is different from that of V1, especially the response at the middle layer (200 mm). Based on the revealed strong correlation between fine-root RAI and suction distribution, this may be caused by the variation of fine-root distribution between V1 and V2.

In previous study on evapotranspiration induced suction, suction decreases along increasing soil depth (Ng et al. 2016; Liu et al. 2019; Ng et al. 2020b). The distribution of RAI of along depth peaks at the middle layer, with the RAI of fine roots and coarse roots not distinguished. In contrast, the RAI of fine roots in this study shows the highest at the lower layer (Fig. 4). This leads to a different pattern of suction distribution from previous studies.

3.5 Effect of root on soil-water characteristics

Fig. 11 shows the variation of the drying soil-water characteristics curve (SWCC) for vegetated soil (V1) as well as bare soil (B) at the same depth for the three periods. Because the SWCC of bare soil B varies very little in the three time periods, the SWCC of V1 (from 04 to 12 September) is used to represent the SWCC of bare soil B in the three time periods. The

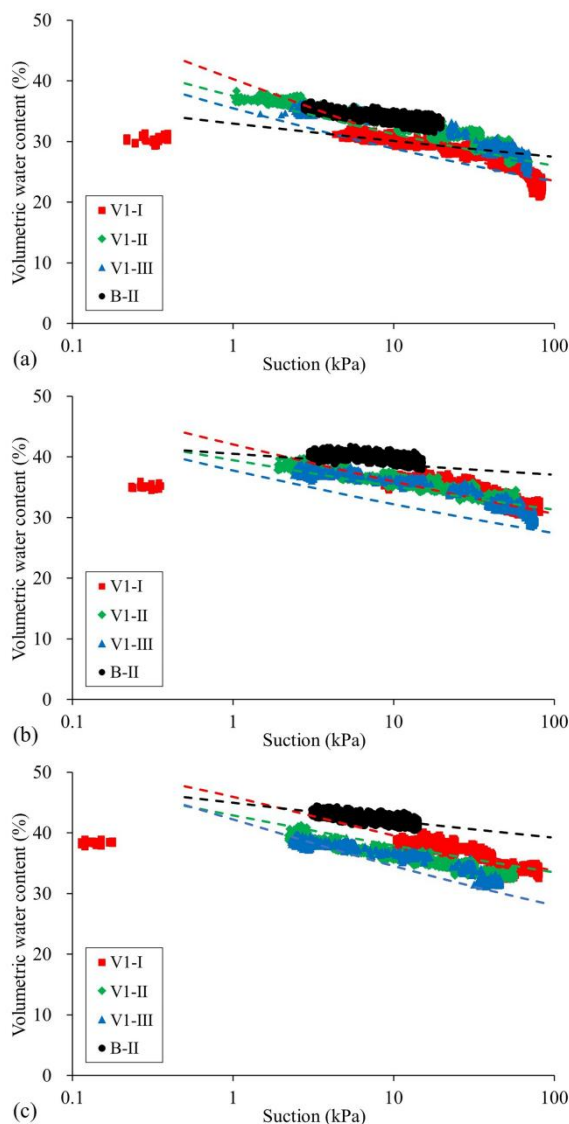


Fig. 11 Measured drying SWCCs along soil depth of bare soil B and vegetated soil V1: (a) at 100 mm; (b) at 200 mm; and (c) at 300 mm. (I) from 25 June to 05 July; (II) from 04 to 12 September; and (III) from 18 September to 01 October (The dashed line is the fitted curve).

drying SWCC of the bare soil is above the vegetated soil, indicating that a higher volumetric water content of the bare soil at the same suction, and a better water retention capacity. The cause of the above phenomenon could be that the root growth causes cracks and formation of large pores (Lu et al. 2020), resulting in a reduced water retention capacity. In addition, the root water uptake is very intensive, which accelerates the drying of soil and formation of cracks. Fine roots have the effects of clogging pores and causing small aggregates to coalesce, which in turn makes the soil structure more compact (Ghestem et al. 2011). Coarse roots cause a relatively large

movement and rearrangement of soil particles and make the soil looser. From the observations in this study, it is obvious that coarse roots have a greater effect in modifying the soil structure than fine roots, and enlarge the soil pore space (Bodner et al. 2014; Lu et al. 2020).

The SWCC is fitted by the empirical equation proposed by van Genuchten (1980)

$$S = \frac{1}{[1 + (a\psi)^n]^m} \quad (2)$$

where, a , m , n are fitting parameters, a is the parameter with air-entry value ($AEV, \psi = \psi_{AEV}$), m and n are shape related parameters; ψ is the matrix suction (kPa); S is the saturation. For convenience, it is advisable to take $m = 1 - 1/n$, the equation contains only two parameters and has a simple form and easy application.

The SWCC fitting parameters were used to calculate the variables of the soil-water characteristic curve, i.e. ψ_{AEV} , desorption rates, saturated volumetric water content (VWC_sat) and residual volumetric water content (VWC_res) (Soltani et al. 2017; Ni et al. 2019; Ng et al. 2022b). Since the SWCCs of vegetated soil V1 is close, the variation of the variables of SWCC is not regular. Moreover, the variation of the suction of bare soil B is small and the data points are few, resulting in large errors in the fitted SWCC (Table 4).

The wetting SWCC of vegetated soil (V1) is demonstrated through the rainfall event, on 11 September (Fig. 12a). The lack of data for three suction curves is due to the removal of outliers from the data. The volumetric water content rises quickly, reaches its peak and then falls to a steady value within 0.5 hour. In contrast, the suction decreases slowly, taking at least 1.5 hours. Fig. 12b shows the characteristics of wetting SWCC (red points) in comparison with the drying SWCC (green points). The wetting SWCC is characterized with an inflection point at about 80 kPa, where a rise of suction happens. On the left of this inflection point, the wetting SWCC is above the drying SWCC, which is physically impossible. This is due to the nature of the 2100F ceramic probe, which requires a longer response time for rising or falling in suction than the soil moisture probe, resulting in suction that does not correspond to the moisture content in real time.

4 Discussion and Research Challenges

4.1 Effect of solar radiation on suction

The suction of vegetated soil V1 increases with the cumulative solar radiation linearly with good correlations, which is significant ($R^2 > 0.9$, $p < 0.001$). The existing models (Indraratna et al. 2006; Nyambayo and Potts 2010; Zhu et al. 2018) for soil-plant-atmosphere interaction mainly adopt vegetation- and soil-related parameters as input.

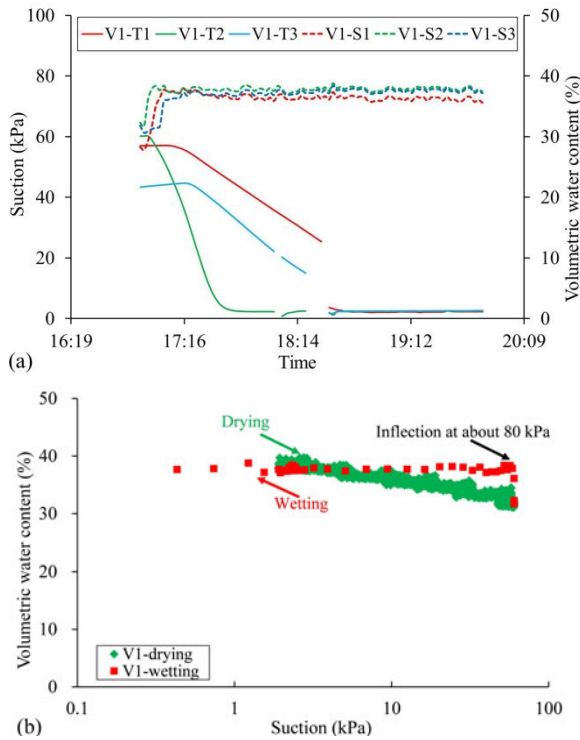


Fig. 12 The drying and wetting SWCCs between 04 and 12 September for vegetated soil V1: (a) changes in suction and volumetric water content subjected to rainfall on 11 September; (b) wetting-drying SWCC at depth of 200 mm (T: Suction; S: Volumetric water content).

While the solar radiation, temperature, and humidity in the atmosphere are ignored, because the relationships between these parameters and suction are not well established. In this study, within the 100 kPa suction range, the relationship between solar radiation and transpiration-induced suction is found. This linear relationship provides an important input for modeling root water uptake in the framework of soil-plant-atmosphere interaction.

However, this relationship is not unconstrained, because the root water uptake intensity would decrease at the high suction range, and root distribution affects the relationship between solar radiation and suction (Fig. 7). In addition to this, it can be seen in Fig. 6d that the increase in solar radiation increases the temperature and decreases the relative humidity. The higher the temperature in a certain range and the lower the relative humidity, the greater the vapor pressure difference inside and outside the leaf, and the easier the water vapor from the stomata to diffuse out, enhancing the transpiration. If the solar radiation is too strong and the temperature is too high, the stomata of leaves will be closed and the transpiration will be weakened. Solar radiation, temperature, and relative humidity affect vegetation transpiration in a coupled manner.

The linear relationship between cumulative radiation and suction could provide an important input in root water uptake models for evaluating slope stability. Yet, this relationship is still not quantified for usage in the numerical models. Further work will focus on the calibration of this linear relationship in an experimental environment, where the parameters such as leaf area index, solar radiation, temperature, humidity, soil water content, and fine root content could be controlled, to isolate the influence of solar

Table 4 Summary of the SWCC variables determined by SWCC fitting parameters

Test			Drying-SWCC variables			
Types	Depth (mm)	Date	Air-entry value (kPa)	Desorption rate (log kPa) ⁻¹	WVC_sat	WVC_res
V1	100	25-Jun. to 05-Jul.	0.0900	-0.19	0.51	0.23
		04-Sep. to 12-Sep.	0.0200	-0.14	0.50	0.27
		18-Sep. to 01-Oct.	0.0200	-0.15	0.50	0.25
	200	25-Jun. to 05-Jul.	0.0400	-0.12	0.51	0.30
		04-Sep. to 12-Sep.	0.0100	-0.09	0.50	0.33
		18-Sep. to 01-Oct.	0.0100	-0.13	0.50	0.29
300	25-Jun. to 05-Jul.	0.1500	-0.13	0.52	0.32	
	04-Sep. to 12-Sep.	0.0300	-0.11	0.51	0.32	
	18-Sep. to 01-Oct.	0.0800	-0.15	0.51	0.27	
B	100	04-Sep. to 12-Sep.	0.0004	-0.15	0.45	0.31
	200	04-Sep. to 12-Sep.	0.0002	-0.04	0.48	0.41
	300	04-Sep. to 12-Sep.	0.0100	-0.06	0.51	0.39

Note: WVC_sat, saturated volumetric water content; WVC_res, residual volumetric water content.

radiation from all other parameters.

4.2 Implication of fine root distribution on shallow landslide along bedrock

Shallow landslides tend to occur on potential slip surfaces near bedrock, where shear strength is the weakest. During rainfall, the bedrock functions as a less permeable layer to reduce the downward seepage of water. As a result, water table will rise and thus reduce the effective stress at the interface. Then the soil layer is prone to slide along the potential slip surface near the bedrock under the action of the gravity-induced driving force.

For those vegetated shallow bedrock slopes (thicknesses < 2 m), plant roots can easily penetrate the soil to reach the bedrock, or be even embedded in bedrock fissures. On one hand, root growth downwards is impeded, which in turn leads to a lot of roots growing near the soil-bedrock interface (as shown in Fig. 13). This can effectively improve the shear strength of the slip surface (Greenway 1987; Stokes et al. 2009). On the other hand, prior to rainfall event, the high concentration of fine roots could substantially reduce the water content and enhance the suction at the interface. As a result, the permeability around the interface is substantially reduced, preventing the pore water pressure to build

up at the interface. The root system (especially fine roots) can greatly alter the soil structure and state of soil saturation, which is conducive for improving the mechanical and hydraulic effects of the vegetated slope and improving the stability of slope (Ng and Menzies 2007; Feng et al. 2020; Lu et al. 2020). The distribution of fine roots and their corresponding suction response in this study can provide a scientific basis for stability assessment of shallow bedrock slopes.

5 Conclusions

Continuous monitoring of soil water content and water potential was conducted for 4 months under natural conditions, on a soil layer vegetated with the shrub species of *Amorpha fruticose*. Accordingly, the effect of solar radiation on suction, as well as the effects of fine-root distribution on suction and soil-water characteristics were quantified, compared, and discussed. The key conclusions can be drawn as follows:

1. Solar radiation determines the intensity of transpiration to a large extent, which further affects the water uptake by plant roots and thus the suction of vegetated soil. A linear relationship between the suction and cumulative solar radiation was found.

However, this linear relationship is not unconstrained, because the root water uptake intensity decreases with increasing suction when a threshold suction of about 100 kPa is exceeded. This linear relationship can provide an important input for modeling root water uptake in the framework of soil-plant-atmosphere interaction.

2. In contrast to previous studies, 5 months after transplantation, the distribution of suction along soil depth shows higher suction values at the lower layer than those at the middle of soil. Fine roots are proved to be the main root class of water uptake in plants. Furthermore, the RAI can be used to characterize the root water

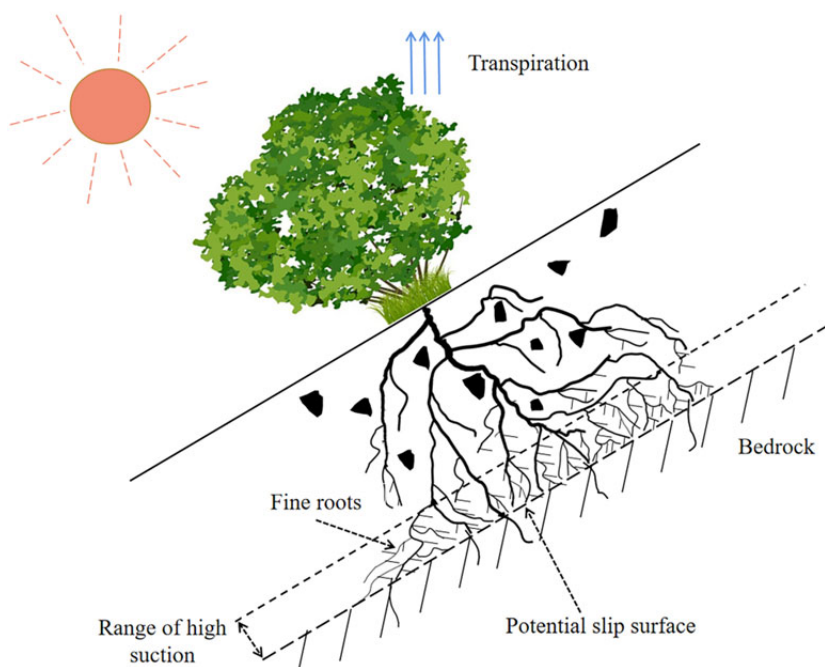


Fig. 13 Schematic diagram of vegetation growing in a relatively shallow soil stratum sitting on a bedrock.

uptake intensity. In this study, the lower layer of soil has the greatest RAI of fine roots and the strongest root water uptake ability, resulting in higher suction at the lower layer.

3. Comparison of SWCCs between bare soil and vegetated soil showed that the volumetric water content of bare soil is higher than that of vegetated soil for the same suction level, which means that bare soil has a greater water retention capacity. Root growth affects the soil pore size distribution. It is postulated that fine and coarse roots tended to make the soil structure more and less compacted as compared with the initial state, respectively. In addition, results implied that coarse roots may have a

greater effect on structural evolution of soils based on observed water retention trends. In other words, it is expected that the overall root system will enlarge the accessible pore population for water exchange and flow.

4. Vegetation growing on slopes with shallow bedrock results in much fine roots near the soil-bedrock interface. Prior to rainfall, high suction would accumulate due to the effect of fine roots at the soil-rock interface. This would further reduce the permeability of unsaturated soil and thus undermine pore pressure buildup at the interface. The risk of shallow slope failure would be reduced accordingly.

Acknowledgments

The authors acknowledge the financial supports from the National Natural Science Foundation of China (grant No. 41925030 and 4179043), the Second Tibetan Plateau Scientific Expedition and Research Program (STEP, grant No. 2019QZKK0904), and the

Natural Science Foundation of Shaanxi Province (2020JQ-041). Technical support from the Yanting Agro-ecological Experiment Station of Purple Soil of Chinese Academy of Sciences is also acknowledged.

References

- Allen RG, Pereira LS, Raes D, et al. (1998) Crop evapotranspiration. Guidelines for Computing Crop Water Requirements. Irrigation and Drainage Paper 56. FAO, Rome, Italy. pp 1-3.
- ASTM (2017) Standard practice for classification of soils for engineering purposes (Unified Soil Classification System). ASTM standard D 2487-17. West Conshohocken, USA. <https://doi.org/10.1520/D2487-17>
- Baille M, Baille A, Laury JC (1994) A simplified model for predicting evapotranspiration rate of nine ornamental species vs. climate factors and leaf area. *Sci Hort* 59(3-4): 217-232. [https://doi.org/10.1016/0304-4238\(94\)90015-9](https://doi.org/10.1016/0304-4238(94)90015-9)
- Bodner G, Leitner D, Kaul HP (2014) Coarse and fine root plants affect pore size distributions differently. *Plant Soil* 380(1-2): 133-151. <https://doi.org/10.1007/s11104-014-2079-8>
- Croissant T, Steer P, Lague D, et al. (2019) Seismic cycles, earthquakes, landslides and sediment fluxes: linking tectonics to surface processes using a reduced-complexity model. *Geomorphology* 339 (12): 87-103. <https://doi.org/10.1016/j.geomorph.2019.04.017>
- Feddes RA, Kowalik PJ, Zaradny H (1978) Simulation of Field Water Use and Crop Yield. Centre for Agricultural Publishing and Documentation.
- Feng S, Liu HW, Ng CWW (2020) Analytical analysis of the mechanical and hydrological effects of vegetation on shallow slope stability. *Comput Geotech* 118. <https://doi.org/10.1016/j.compgeo.2019.103335>
- Ghestem M, Sidle RC, Stokes A (2011) The influence of plant root systems on subsurface flow: Implications for slope stability. *BioScience* 61(11): 869-879. <https://doi.org/10.1525/bio.2011.61.11.6>
- Grayston SJ, Vaughan D, Jones D (1997) Rhizosphere carbon flow in trees, in comparison with annual plants: the importance of root exudation and its impact on microbial activity and nutrient availability. *Appl Soil Ecol* 5(1): 29-56. [https://doi.org/10.1016/S0929-1393\(96\)00126-6](https://doi.org/10.1016/S0929-1393(96)00126-6)
- Greenway DR (1987) In: Richards MG (ed) Slope stability: geotechnical engineering and geomorphology. Vegetation and slope stability. pp 187-230.
- Haseba T, Takechi O (1972) Studies of transpiration in relation to the environment. *J Agric Meteorol* 28(2): 93-101. <https://doi.org/10.2480/agrmet.28.93>
- Indraratna B, Fatahi B, Khabbaz H (2006) Numerical analysis of matric suction effects of tree roots. *P I Civil Eng-Geotec* 159(2): 77-90. <https://doi.org/10.1680/jgeot.2006.159.2.77>
- Jin HF, Shi DM, Zeng XY, et al. (2019) Mechanisms of root-soil reinforcement in bio-embankments of sloping farmland in the purple hilly area, China. *J Mt Sci* 16(10): 2285-2298. <https://doi.org/10.1007/s11629-019-5476-x>
- Jotisankasa A, Sirirattanachat T (2017) Effects of grass roots on soil-water retention curve and permeability function. *Can Geotech J* 54(11): 1612-1622. <https://doi.org/10.1139/cgj-2016-0281>
- Lin JY, Lin CH, Tsay YS (2016) A model for prediction evapotranspiration rate of wild allamanda for living wall systems. Conference: Indoor Air, Ghent, Belgium.
- Liu Q, Su L, Xia Z, Liu D, et al. (2019) Effects of soil properties and illumination intensities on matric suction of vegetated soil. *Sustainability* 11(22). <https://doi.org/10.3390/su11226475>
- Lu J, Zhang Q, Werner AD, et al. (2020) Root-induced changes of soil hydraulic properties – A review. *J Hydrol* 589(1-2). <https://doi.org/10.1016/j.jhydrol.2020.125203>
- Mu QY, Dong H, Liao HJ, et al. (2020) Water-retention curves

- of loess under wetting–drying cycles. *Geotech Lett* 10(2): 135-140. <https://doi.org/10.1680/jgele.19.00025>
- Mu QY, Dong H, Liao HJ, Zhou, et al. (2022) Effects of in situ wetting–drying cycles on the mechanical behaviour of an intact loess. *Can Geotech J* 59(7): 1281-1284. <https://doi.org/10.1139/cgj-2020-0696>
- Ng CWW, Pang YW (2000) Experimental investigations of the soil-water characteristics of a volcanic soil. *Can Geotech J* 37(6): 1252-1264. <https://doi.org/10.1139/cgj-37-6-1252>
- Ng CWW, Menzies B (2007) *Advanced Unsaturated Soil Mechanics and Engineering*. Taylor & Francis. CRC Press, London, UK. <https://doi.org/10.1201/9781482266122>
- Ng CWW, Ni JJ, Leung AK, et al. (2016) Effects of planting density on tree growth and induced soil suction. *Géotechnique* 66(9): 711-724. <https://doi.org/10.1680/jgeot.15.P.196>
- Ng CWW (2017) Atmosphere-plant-soil interactions: theories and mechanism. *Chinese J Geotechnical Eng* 39(1): 1-47. (In Chinese) <https://doi.org/10.11779/CJGE201701001>
- Ng CWW, Sadeghi H, Jafarzadeh F, et al. (2020a) Effect of microstructure on shear strength and dilatancy of unsaturated loess at high suctions. *Can Geotech J* 57(2): 221-235. <https://doi.org/10.1139/cgj-2018-0592>
- Ng CWW, Ni JJ, Leung AK (2020b) Effects of plant growth and spacing on soil hydrological changes: a field study. *Géotechnique* 70(10): 867-881. <https://doi.org/10.1680/jgeot.18.P.207>
- Ng CWW, Guo HW, Ni JJ, et al. (2022a) Effects of soil-plant-biochar interactions on water retention and slope stability under various rainfall patterns. *Landslides* 19(6): 1379–1390. <https://doi.org/10.1007/s10346-022-01874-y>
- Ng CWW, Zhang Q, Zhou C, et al. (2022b) Eco-geotechnics for human sustainability. *Sci China Tech Sci* 65: 2809–2845. <https://doi.org/10.1007/s11431-022-2174-9>
- Ni JJ, Leung AK, Ng CWW, et al. (2018) Modelling hydro-mechanical reinforcements of plants to slope stability. *Comput Geotech* 95: 99-109. <https://doi.org/10.1016/j.compgeo.2017.09.001>
- Ni JJ, Leung A, Ng CWW (2019) Modelling effects of root growth and decay on soil water retention and permeability. *Can Geotech J* 56(7): 1049–1055. <https://doi.org/10.1139/cgj-2018-0402>
- Nyambayo VP, Potts DM (2010) Numerical simulation of evapotranspiration using a root water uptake model. *Comput Geotech* 37(1-2): 175-186. <https://doi.org/10.1016/j.compgeo.2009.08.008>
- Pieruschka P, Huber G, Berry JA (2010) Control of transpiration by radiation. *PNAS* 107(30): 13372-7. <https://doi.org/10.1073/pnas.0913177107>
- Pollen N, Simon A, Collison A (2004) Advances in assessing the mechanical and hydrologic effects of riparian vegetation on streambank stability. In *Riparian Vegetation and Fluvial Geomorphology*. pp 125-139. <https://doi.org/10.1029/008wsa10>
- Rajamanthri K, Jotisanakasa A, Aramrak S (2021) Effects of *Chrysopogon zizanioides* root biomass and plant age on hydro-mechanical behavior of root-permeated soils. *Int J Geosynth Groun* 7(2). <https://doi.org/10.1007/s40891-021-00271-0>
- Rickli C, Graf F (2009) Effects of forests on shallow landslides - case studies in Switzerland. *For Snow Landsc Res* 82 (1): 33-44.
- Romero E, Gens A, Lloret A (1999) Water permeability, water retention and microstructure of unsaturated compacted Boom clay. *Eng Geol* 54(1-2): 117-127. [https://doi.org/10.1016/S0013-7952\(99\)00067-8](https://doi.org/10.1016/S0013-7952(99)00067-8)
- van Genuchten, MT (1987) A numerical model for water and solute movement in and below the root zone. Research Report No.121. U.S. Salinity laboratory, USDA, ARS, Riverside, Calif.
- Sadeghi H, Chiu AC, Ng CWW, et al. (2020) A vacuum-refilled tensiometer for deep monitoring of in-situ pore water pressure. *Sci Iran* 27(2): 596-606. <https://doi.org/10.24200/sci.2018.5052.1063>
- Sadeghi H, Hossen SB, Chiu SB, et al. (2016) Water retention curves of intact and re-compacted loess at different net stresses. *Jpn Geotech Soc Spec Publ* 2(4): 221-225. <https://doi.org/10.3208/jgssp.HKG-04>
- Sadeghi H, Ng CWW (2018) Shear behaviour of a desiccated loess with three different microstructures. In 7th International conference on unsaturated soils. <https://doi.org/10.13140/RG.2.2.18419.17447>
- Scanlan CA, Hinz C (2010) Insight into the processes and effects of root induced changes to soil hydraulic properties. 19th World Congress of Soil Science, Soil Solutions for a Changing World, Brisbane, Australia, 1–6 August 2010. pp 41–44.
- Scholl P, Leitne D, Kammerer G, et al. (2014) Root induced changes of effective 1D hydraulic properties in a soil column. *Plant Soil* 381(1-2): 193-213. <https://doi.org/10.1007/s11104-014-2121-x>
- Segal E, Kushnir T, Mualem Y, et al. (2008) Water Uptake and Hydraulics of the Root Hair Rhizosphere. *Vadose Zone J* 7(3): 1027-1034. <https://doi.org/10.2136/vzj2007.0122>
- Singh DP, Turne NC, Rawson HM (1982) Effects of radiation, temperature and humidity on photosynthesis, transpiration and water use efficiency of oilseed rape (*Brassica campestris* L.). *Biol Plantarum* 24(2): 130-135. <https://doi.org/10.1007/BF02902859>
- Soltania A, Azimib M, Deng A, et al. (2017) A simplified method for determination of the soil–water characteristic curve variables. *Int J Geotech Eng* 13(9): 316-325. <https://doi.org/10.1080/19386362.2017.1344450>
- Stokes A, Atger C, Bengough AG, et al. (2009) Desirable plant root traits for protecting natural and engineered slopes against landslides. *Plant Soil* 324(1-2): 1-30. <https://doi.org/10.1007/s11104-009-0159-y>
- Su LJ, Hu BL, Xie QJ, et al. (2020) Experimental and theoretical study of mechanical properties of root-soil interface for slope protection. *J Mt Sci* 17(11): 2784-2795. <https://doi.org/10.1007/s11629-020-6077-4>
- Ta H, Shin JH, Ahn TI, et al. (2011) Modeling of transpiration of paprika (*Capsicum annum* L.) plants based on radiation and leaf area index in soilless culture. *Hortic Environ Biote* 52(3): 265-269. <https://doi.org/10.1007/s13580-011-0216-3>
- Traoré O, Groleau-Renaud, V, Plantureux S, et al. (2000) Effect of root mucilage and modelled root exudates on soil structure. *Eur J Soil Sci* 51(4): 575-581. <https://doi.org/10.1111/j.1365-2389.2000.00348.x>
- Waldron LJ (1977) The Shear Resistance of Root-Permeated Homogeneous and Stratified Soil. *Soil Sci Soc Am J* 41(5): 843-849. <https://doi.org/10.2136/sssaj1977.03615995004100050005x>
- Zhang CB, Liu YT, Li DR, et al. (2020) Influence of soil moisture content on pullout properties of *Hippophae rhamnoides* Linn. roots. *J Mt Sci* 17(11): 2816-2826. <https://doi.org/10.1007/s11629-020-6072-9>
- Zhu H, Zhang LM, Garg A (2018) Investigating plant transpiration-induced soil suction affected by root morphology and root depth. *Comput Geotech* 103: 26-31. <https://doi.org/10.1016/j.compgeo.2018.06.019>